Journal of Power Sources 256 (2014) 312–318

Contents lists available at ScienceDirect

Journal of Power Sources

journal homepage: www.elsevier.com/locate/jpowsour

Electrocatalytic performance enhancement of $La_{0.6}Sr_{0.4}Co_{0.2}Fe_{0.8}O_{3-\delta}$–$Y_2O_3$ stabilized ZrO_2 cathodes prepared by an impregnation technique

Jing Chen [a,b], Yihui Liu [a], Bo Chi [a], Jian Pu [a], Jian Li [a,*]

[a] Center for Fuel Cell Innovation, School of Materials Science and Engineering, State Key Laboratory of Material Processing and Die & Mould Technology, Huazhong University of Science and Technology, 1037 Luoyu Rd, Wuhan, Hubei 430074, PR China
[b] School of Chemistry and Chemical Engineering, Henan University of Technology, Zhengzhou 450001, PR China

HIGHLIGHTS

- Optimization of the half cell performance by the LSCF loadings and LSCF particle morphology.
- Novel surfactant was introduced in the precursor solution.
- *N*-ethyl-perfluoyooctylsulfonamide had a great effect on the performance of LSCF-YSZ cathodes.

ARTICLE INFO

Article history:
Received 10 November 2013
Received in revised form
3 January 2014
Accepted 19 January 2014
Available online 24 January 2014

Keywords:
Cathodes
Impregnation
Loading
Surfactants
Electrocatalytic performance

ABSTRACT

The electrocatalytic performance of the oxygen-reduction reaction of $La_{0.6}Sr_{0.4}Co_{0.2}Fe_{0.8}O_{3-\delta}$ (LSCF) $-Y_2O_3$ stabilized ZrO_2 (YSZ) cathodes prepared by an impregnation technique has been investigated as cathodes for intermediate temperature solid oxide fuel cells. The electrocatalytic activity of LSCF-YSZ cathodes increases with the introduction of LSCF phases to the YSZ scaffold. The introduction of surfactants into LSCF-precursor solutions during preparation has a great effect on the microstructure and electrochemical performance of LSCF-YSZ composite cathodes. *N*-ethyl-perfluoyooctylsulfonamide (DF10) is a type of commonly used nonionic flusurfactant which affects the LSCF particles' morphology on the YSZ scaffold. Using *N*-ethyl-perfluoyooctylsulfonamide (DF10) + acetylacetone during the preparation of LSCF-YSZ composite cathodes decreases the electrode polarization resistance (R_e) of cathodes from 0.45 to 0.18 Ω cm^2. We obtained a notable improvement in the electrochemical performance of LSCF-YSZ-composite cathodes with uniform and continuous LSCF particle distribution on the surface of YSZ scaffold.

1. Introduction

(La, Sr)(Co, Fe)O_3 (LSCF) perovskite oxides are widely accepted as the ideal cathode material for solid oxide fuel cells (SOFCs) that operate in the intermediate temperature range (between 600 and 800 °C) [1,2]. However, the reaction between LSCF and Y_2O_3-stabilized ZrO_2 (YSZ) electrolytes under operating conditions is an obstacle to commercial application [3]. Moreover, high operating temperature results in higher system costs as well as increased performance degradation rates; high temperatures also slow start-up and shutdown cycles [4]. To improve performance stability, lower the cost of SOFCs, and ameliorate the problem of slowed start-up and shutdown cycles, the operating temperature should be reduced to as low as about 700 °C [4]. However, the decrease in catalytic activity for oxygen-reduction reactions caused by lowering operating temperatures must be achieved in order to develop high-performance cathodes. Introduction of a small amount of catalyst into LSCF cathodes can promote their catalytic activity [5]. Meanwhile, adding ionic-conducting phases such as Gd-doped CeO_2 (GDC) [6] or Sm-doped CeO_2 (SDC) [7] to LSCF cathodes can also improve their electrochemical performance.

Wet impregnation is an effective method that avoids the difficulties encountered in the preparation of cathodes using conventional methods. Conventional methods introduce either catalyst or electrolyte materials into the pre-formed electrolyte or catalyst scaffolds on the dense electrolytes [8–11]. Recently, wet impregnation has been used for the development of LSCF-impregnated YSZ (LSCF-YSZ) [12,13], and LSCF-impregnated GDC (LSCF-GDC) cathodes [14–16]. In particular, Pd particles can be incorporated into LSCF- [16] or Sr-doped $LaMnO_3$ cathodes (LSM) [17] to improve their electrocatalytic activities. Jiang [9] and Vohs and Gorte [8] have thoroughly reviewed the progress in the application both in

* Corresponding author.
E-mail address: lijian@hust.edu.cn (J. Li).

0378-7753/$ – see front matter © 2014 Elsevier B.V. All rights reserved.
http://dx.doi.org/10.1016/j.jpowsour.2014.01.081

cathodes and anodes, and discussed the advances and challenges in the development of nanoscale and nano-structure electrode.

Here, we created LSCF-YSZ cathodes by impregnating LSCF phases into porous YSZ scaffolds. We furthermore investigated the effects of microstructure on the catalytic performance of cathodes by measuring its electrochemical performance and microstructure characterization. Lastly, we examined the effects of LSCF loadings and surfactants on microstructure, and electrocatalytic activities of LSCF-YSZ cathodes. Our results reveal that the increase in LSCF loadings improves the electrochemical performance of LSCF-YSZ cathodes and that the introduction of surfactants, such as DF10 + acetylacetone, can optimize the performance of the cathode.

2. Experimental

The YSZ electrolyte substrates were prepared by first sintering die-pressed disks of 8% mol YSZ powder (TZ-8YS, Tosoh, Japan) at 1500 °C for 4 h in air, and then subjecting them to mechanical polishing. The substrate disks were 21 mm in diameter and 1.2 mm in thickness. To establish YSZ-porous layer on the dense YSZ electrolyte, 26 nm YSZ slurry (TZ-8Y, Tosoh, Japan) was prepared and applied to the YSZ electrolyte disks by screen printing. This procedure was followed by sintering at 1200 °C for 1 h in air. The thickness of the porous YSZ layer was about 10 μm and the active electrode area was 0.5 cm^2.

An aqueous solution of the LSCF precursor was prepared from $La(NO_3)_3 \cdot 6H_2O$, $Sr(NO_3)_2$, $Co(NO_3)_2 \cdot 6H_2O$, and $Fe(NO_3)_3 \cdot 9H_2O$ (Sinopharm Chemical Reagent Co. Ltd., Shanghai, China) at a molar ratio of La: Sr: Co: Fe = 6:4:2:8 and surfactants. Table 1 lists the names and amounts of surfactants that were used in the LSCF solution as well as the name of half cells. Impregnation treatment was carried out by dropping LSCF solution onto the surface of the porous YSZ layer under ultrasonic treatment for 10 min, and followed the impregnated samples were dried in air and then heated to 800 °C in air for 1 h to obtain the LSCF phase. LSCF loading can be recorded by measuring the weight gain of the sample before and after impregnation treatment. The process is then repeated until the desired LSCF loading is reached.

Pt paste was painted on top of the cathode and served as a current collector. It was also painted onto the opposite side of the electrolyte disc to form both the counter and reference electrodes. The counter electrode was positioned symmetrically to the work electrode (LSCF cathode) and the reference electrode was painted in a ring at the edge of the electrolyte substrate. The gap between the counter electrode and the reference electrode was at least 4 mm, which was three times larger than the thickness of the electrolyte [18].

The electrochemical impedance spectra and polarization curves of the electrodes were obtained in the three-electrode configuration [19] at a temperature of between 600 °C and 750 °C, with an impedance–gain phase analyzer (Solartron 1260) and an electrochemical interface (Solartron 1287) at open-circuit. A Sirion 200 scanning electron microscope (SEM) was employed to examine the microstructure and distribution of impregnated LSCF nanoparticles.

Table 1
The names and amounts of surfactants used in the LSCF solution.

	The names of surfactants	Amount (wt.%)	The number of half-cell
1	Pluronic F127	1.5	F127
2	Polyvinylpyrrolidone (PVP)	1.5	PVP
3	*N*-ethyl-perfluoyooctylsulfonamide DF-10)	0.5	DF10
4	Acetylacetone + DF-10	1.0 + 0.5 (DF-10)	DF10 + acetylacetone
5	Without surfactant	0	No

3. Results and discussion

3.1. Effects of LSCF loadings on cathode performance

Electrochemical performance of LSCF-YSZ cathodes with different LSCF loadings was characterized by the electrode polarization resistance (R_e) and the activation energy of the oxygen reduction reactions at different temperatures. The value of R_e decrease rapidly with the increase of LSCF loadings (Fig. 1a) and this trend was dramatic in lower temperature ranges between 600 and 650 °C. At 600 °C, the R_e of the LSCF-YSZ cathode was 12.4 Ω cm^2 with an LSCF loading of 0.2 mg cm^{-2}. However, R_e decreased to 0.59 Ω cm^2 as the LSCF loading reached 1.1 mg cm^{-2}, the value of which was 1/21 compared to the value of the cathode with LSCF loading of 0.2 mg cm^{-2}. When the operating temperature increased to 750 °C, the value of R_e were 0.55 and 0.048 Ω cm^2 with LSCF loadings of 0.2 and 1.1 mg cm^{-2}, respectively. The LSCF loadings significantly affect the polarization resistance of the cathodes. The R_e values are considered to be very low in comparison to those obtained with pure LSCF cathodes at 726 °C, where R_e values of 0.236 Ω cm^2 [20] were reported. LSCF loading increased to

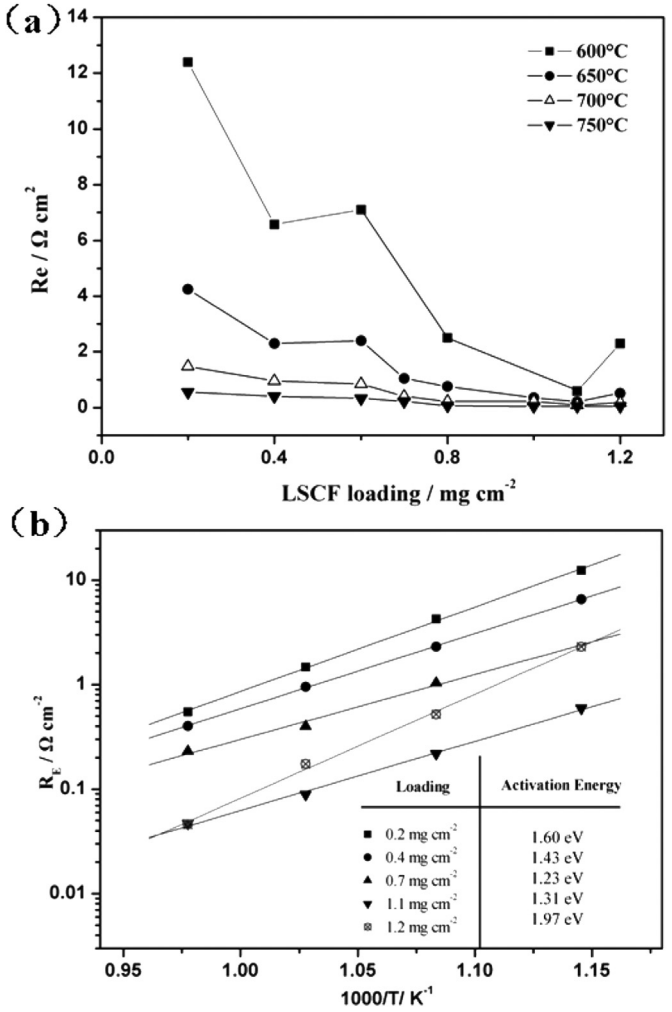

Fig. 1. (a) Effect of the impregnated LSCF loading on the electrode polarization resistance of LSCF-YSZ composite cathodes at different temperatures and (b) the activation energy of the oxygen reduction reactions on LSCF-YSZ composite cathodes.

1.2 mg cm^{-2}, and the value of R_e decreased in Fig. 1a, which indicate the change of the primary rate-limiting mechanism for oxygen reduction reaction. The catalytic properties of composite cathodes are closely related to the relative proportion of two materials comprising the composite, which result from the difference in the ratio of grain size of LSCF to that of YSZ. The study on micro-modeling of LSM-YSZ composite electrode showed that the optimal YSZ volume fraction ($ø_{YSZ}$) with minimum polarization resistance depends on the ratio of average grain size of YSZ (r_{io}) to that of LSM (r_{el}), varying from $ø_{YSZ} = 0.24$ for $r_{io}/r_{el} = 0.2$ to $ø_{YSZ} = 0.55$ for $r_{io}/r_{el} = 1$ and $ø_{YSZ} = 0.81$ for $r_{io}/r_{el} = 5$ [21]. In this paper, only low LSCF content was discussed, the reason was that R_e was difficult to distinguish in impedance spectra following the appearance of the inductive loop [22] in the fourth quadrant with the increase of the LSCF loading, which was discussed in another paper.

The mechanism of oxygen reduction reaction for LSCF electrode was further studied by experimentation or simulation [20,23–25]. Jiang [23] compared the behavior of LSCF electrodes in the absence and presence of gaseous chromium species under current load, and conclude that both surface and bulk diffusion processes are important and occurred in parallel to the electrochemical oxygen reduction reaction. The steps of dissociative adsorption and surface diffusion of oxygen were most significant, and therefore the TPB area was important for O_2 reduction. However, the bulk diffusion process plays a more dominant role on porous LSCF electrodes. Fleig et al. [24] has modeled the behavior of MIEC cathode material using multi-dimensional finite element simulations depending on the polarization resistance on surface reaction coefficient, ionic conductivity and particles size. Depending on these parameters different parts of the cathode are involved in the oxide ion transport to the electrolyte from a very small region close to TPB for a fast surface reaction up to the entire cathode for a very slow surface reaction. For the LSCF-YSZ composite cathode, the LSCF particle size was between 40 and 70 nm, which was smaller than the MIEC particle diameter in the model. According to the model, we predict that the active zone for oxygen reduction is not only the TPB area but also the whole LSCF particles. Increasing the LSCF loading, R_e significantly decreases. The changes of R_e may be closely related to the increasing of the active zone for oxygen reduction which affect the surface path and the bulk path. However, R_e in the impedance spectra was difficult to identify with increasing the content of LSCF loadings because of the appearance of the inductive loop in the fourth quadrant in impedance spectra. The appearance of inductive loop indicates that the primary rate-limiting mechanism has changed from the surface and bulk diffusion processes to the diffusion process of oxygen molecular on the small pore between the LSCF particles. The LSCF-YSZ-cathode performance with LSCF loading can also be described by the activation energy of the oxygen reduction reaction (Fig. 1b).

Fig. 1b shows the temperature dependence of the polarization resistance values for different LSCF loadings. As seen, the activation energy was 1.60, 1.43, 1.23, 1.31, and 1.97 eV for reactions on LSCF-YSZ cathodes with LSCF loading values of 0.2, 0.4, 0.7, 1.1, and 1.2 mg cm^{-2}, respectively. Increasing the LSCF-loading value from 0.2 to 0.7 mg cm^{-2} resulted in a continuous decrease in activation energies (1.60–1.23 eV). This decrease indicates an improvement in cathode performance. However, continuously increasing the LSCF loading from 0.7 to 1.2 mg cm^{-2} led to a corresponding increase in the activation energy (1.23–1.97 eV). The substantially higher activation energy for LSCF loading (1.2 mg cm^{-2}) suggests that a different reaction mechanism was the limiting factor in this reaction.

Polarization curves of the LSCF-YSZ-composite cathodes with different LSCF loadings at 750 °C in air are shown in Fig. 2a. We observed that the overpotential of the LSCF-YSZ cathode increased as the current density increased. In general, the polarization curve is a linear relationship with low current density for LSCF loadings of 0.2 and 0.4 mg cm^{-2}. However, the overpotential decreased as the LSCF loadings increased. Results in Fig. 2a indicated that the step-by-step catalytic process can be observed as one increases the LSCF loadings, and the polarization curves can be separated into three parts when LSCF loading values are 0.6 and 0.8 mg cm^{-2}.

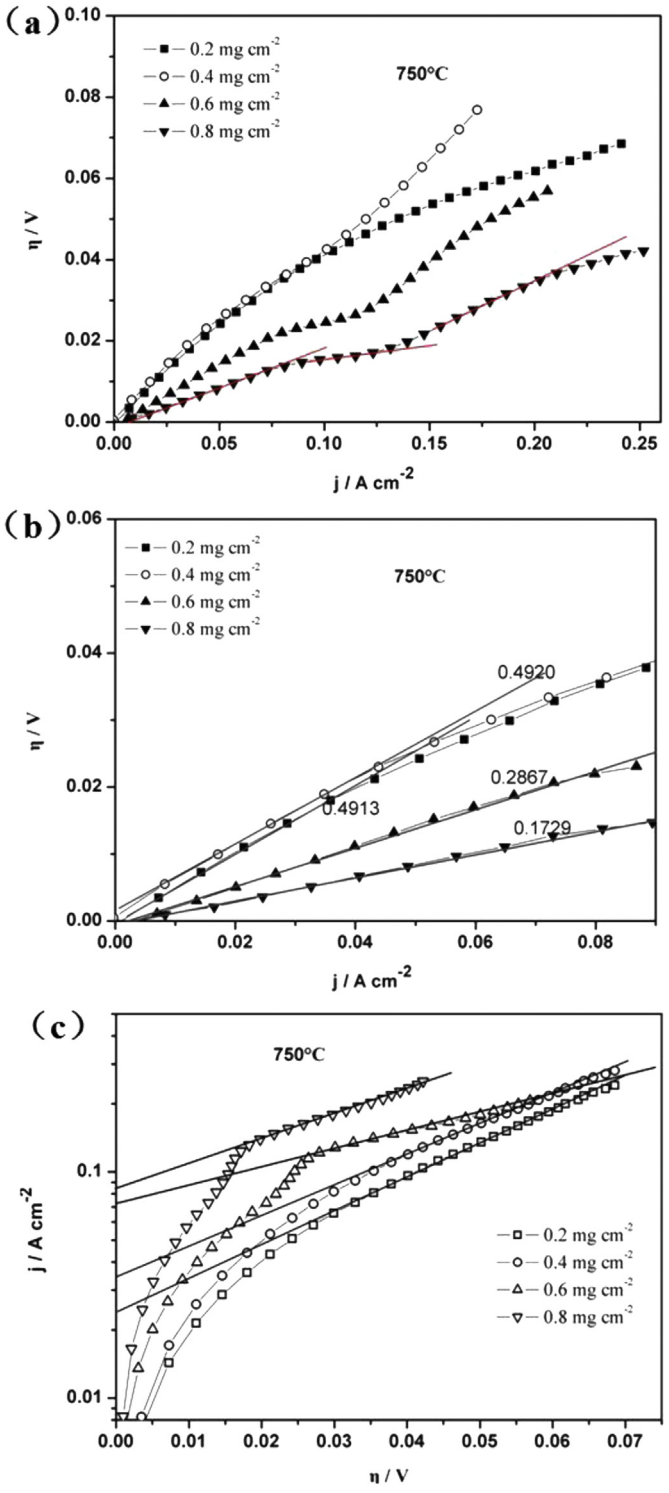

Fig. 2. Polarization curves of the LSCF-YSZ composite cathodes with different LSCF loadings at 750 °C in air: (a) total curves, (b) at low current density regime, (c) at high current density regime.

The Butler–Volmer equation describes a quantitative relationship between the current density (i) and the cathodic activation polarization, or overpotential (η) (Equation (1)).

$$i = i_0\left\{\exp\left(\frac{\beta zF\eta}{RT}\right) - \exp\left(-\frac{(1-\beta)zF\eta}{RT}\right)\right\} \quad (1)$$

where β is a dimensionless, positive number, which is known as the transfer coefficient; i_0 and i are known as the exchange-current density and net-current density, respectively; z is the charge magnitude of the ion; F is the Faraday constant; R is the gas constant; and T is the absolute temperature. Note that the relationship between η and i is nonlinear and implicit; that is, it does not allow an explicit determination of η as a function of the current density. The relationship between the cathodic activation polarization and the current density is nonlinear, except at very low current densities. At the low current density limit, $|\beta zF\eta/RT| \ll 1$ and $|(1-\beta)zF\eta/RT| \ll 1$, the Butler–Volmer equation can be simplified to:

$$|\eta| \approx \frac{RT}{zFi_0} i \quad (2)$$

An important point to note here is that a linear relationship between η and the current density (i) in the low current density limit does not imply an ohmic relationship. Polarization curves at a low current density regime can be linear fitted (see Fig. 2b). The exchange current density (i_0) can be obtained by the following equation [20]:

$$i_0 = \frac{RTi}{zF\eta} = \frac{RT}{zF} \times (\text{Gradient of lines}) \quad (3)$$

Meanwhile, in the high current density regime, $|\beta zF\eta/RT| \gg 1$, the Butler–Volmer equation can be approximated by the Tafel equation, where

$$\eta \approx \frac{RT}{\beta zF}\ln i_0 - \frac{RT}{\beta zF}\ln i \approx a + b\ln i \quad (4)$$

Polarization curves at the high current density regime can be linear fitted according

$$\log i = \log i_0 - \frac{\beta zF}{2.303RT}\eta \quad (5)$$

The exchange current density (i_0) can be obtained following Fig. 2c. The exchange-current density is proportional to the reaction rate and responds directly to the electrode reaction rate [25]. Calculations based on Fig. 2b and c are listed in Table 2. As seen, i_0 increased with the increase of LSCF loadings at both high and low current density regimes, indicating that the introduction of LSCF phases improved the electrocatalytic activities of LSCF-YSZ cathodes, which in turn accelerated the electrochemical reaction on the cathodes. In addition, the value of i_0 at a high current density regime was much greater than that at a low current–density regime, suggesting that the electrochemical reaction at the high current density regime is much faster.

Table 2
Exchange current densities of LSCF-YSZ composite cathodes with different LSCF loadings at 750 °C in air.

LSCF loading (mg cm^{-2})	Exchange current density	
	Low current density regime	High current density regime
0.2	89.7	1055.3
0.4	89.6	1081.5
0.6	153.7	1175.5
0.8	254.9	1213.8

3.2. Effects of LSCF particle morphology on electrocatalytic activity

Generally, the distribution uniformity and the adsorbability of impregnated particles are both important for the microstructure of composite cathodes [10]. Optimizing LSCF loading is an effective strategy for obtaining composite cathodes with uniform microstructures and high electrocatalytic activities. In addition, adding a surfactant to the precursor solution is also widely adopted. Previous studies showed that the addition of the surfactant Triton-X100 to LSM-impregnated YSZ cathodes [26], glycine to LSM-impregnated YSB cathodes [27,28], or ethanol to $Sm_{0.6}Sr_{0.4}CoO_{3-\delta}$ (SSC)-impregnated LSCF cathodes [29] increased the uniformity of introduced nanoparticles and hence enhanced the performance of composite cathodes. Here, we introduced different surfactants into an aqueous nitrate solution of LSCF precursors during LSCF-YSZ cathode fabrication. The electrochemical impedance spectra of LSCF-YSZ-composite cathodes impregnated with LSCF solution by different surfactants are shown in Fig. 3. In these experiments, each sample had 0.4 mg cm^{-2} of LSCF loading. The shapes of electrochemical impedance spectra of cathodes with different surfactants are similar. All are flattened semicircles at 700–750 °C. All spectra are also characterized by an inductance loop in the fourth quadrant, which have been previously reported [30,31]. The R_e of LSCF-YSZ composite cathodes with different surfactants varied, indicating that the surfactants greatly affected the electrocatalytic performance of cathodes (Fig. 3). The R_e of cathodes with N-ethyl-

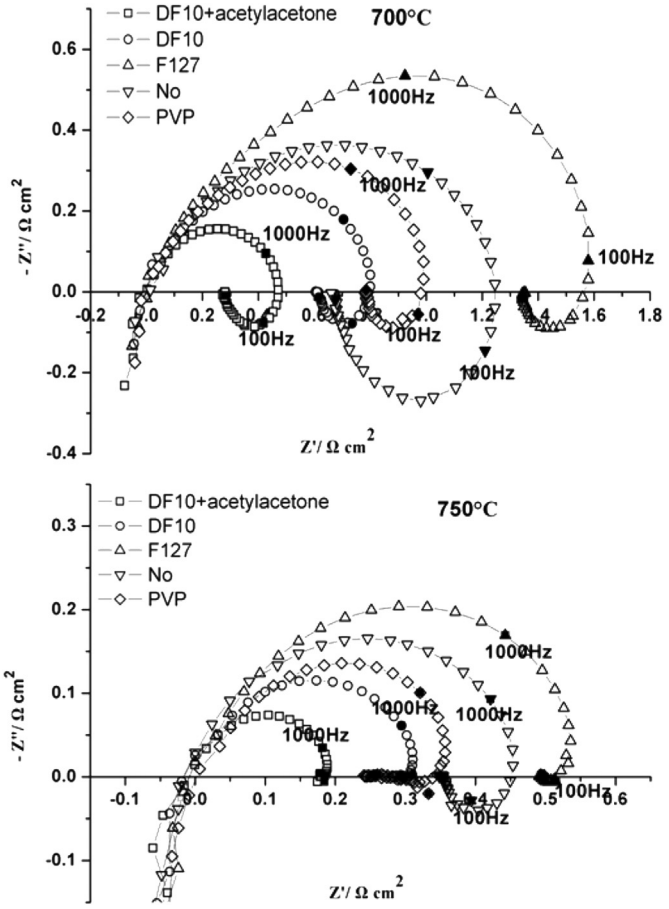

Fig. 3. Electrochemical impedance spectra of the nano-structured LSCF-YSZ composite cathode impregnated with nitrate solution with different surfactants.

perfluoyooctylsulfonamide (DF10), DF10 + acetylacetone, and polyvinylpyrrolidone (PVP) was smaller than that of cathodes without surfactants in the precursor solutions at 700–750 °C. This demonstrates that the introduction of the above-mentioned surfactants we tested improve the electrochemical performance of LSCF-YSZ composite cathodes. However, the effect of pluronic F127 (F127) was much different from other surfactants. After the introduction of F127 during the preparing processes, the R_e of the cathodes increased, suggesting that F127 is able to degrade the electrochemical performance of LSCF-YSZ composite cathodes. The improvement of DF10 + acetylacetone on the electrochemical performance of LSCF-YSZ composite cathodes was the greatest of the four surfactants we evaluated, as indicated by the R_e of the cathodes being reduced from 0.45 to 0.18 Ω cm^2 (due to the introduction of DF10 + acetylacetone). Similarly, the polarization curves of the LSCF-YSZ-composite cathodes were improved by impregnation by LSCF-nitrate solution with different surfactants (Fig. 4). The overpotentials of cathodes are much different at the same current density from 700 to 750 °C. In particular, the overpotentials of cathodes with DF10 + acetylacetone were smaller than those of other surfactants, indicating that the introduction of DF10 + acetylacetone has the greatest improvement on the electrochemical performance of LSCF-YSZ-composite cathodes. These results are also supported by what is shown in Fig. 3.

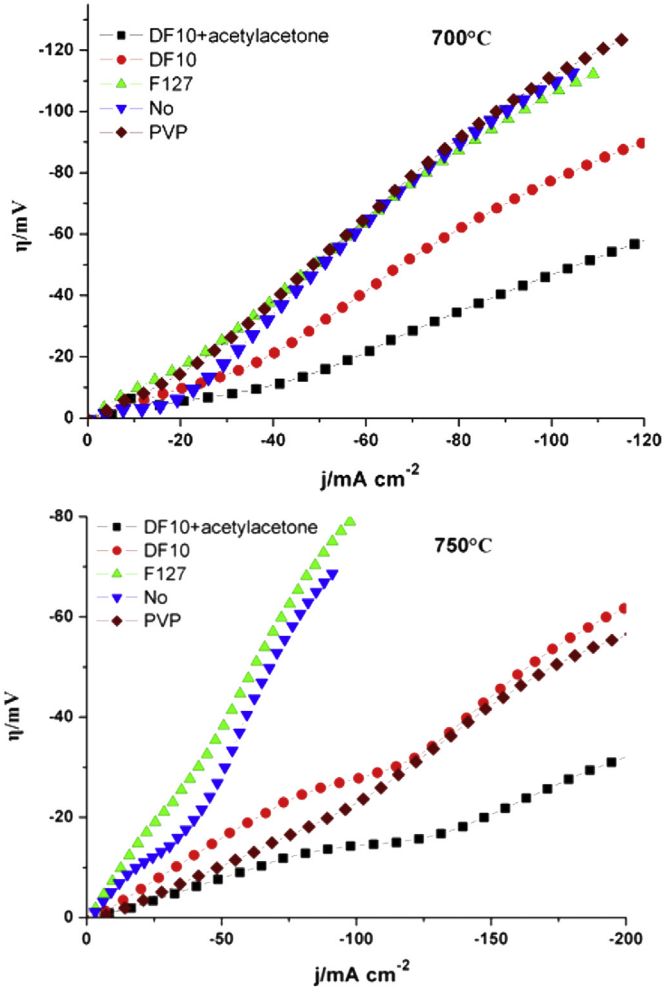

Fig. 4. Polarization curves of the LSCF-YSZ composite cathodes impregnated with nitrate solution with different surfactants.

The density at high and low current density regimes is calculated according to Equations (4) and (5) (Table 3). The exchange current density was greatly affected by the testing temperature, the current density regime, and the surfactant. The exchange current density was higher at 750 °C than at 700 °C for both high- and low-current density regimes. The value of i_0 was greatly affected by the surfactant at the low-current density regime; eg, the value of i_0 at 700 °C was 53 mA cm^{-2} when the electrode prepared with no surfactant assistance. Furthermore, i_0 was 92 mA cm^{-2} and 162 mA cm^{-2} for the cathodes prepared with DF-10 and acetylacetone assistance, respectively. However, i_0 was little affected by the surfactant during the high-current density regime; that is, the value of i_0 at 700 °C was 1064 mA cm^{-2} without the surfactant (No) and 1107 mA cm^{-2} for the cathode prepared by DF-10 + acetylacetone. These results indicate that using a surfactant can significantly affect the electrochemical reaction rate of the electrode at the low-current-density regime. However, at the high-current-density regime, the surfactants we used had no significant effect on the electrochemical reaction rate.

To further understand the effect of the introduction of surfactants into LSCF-precursor solutions on the microstructure of LSCF-YSZ composite cathodes, SEM was employed and the results are shown in Fig. 5. When we examined the cathode prepared by the LSCF-precursor solution without surfactant, irregular spheres of LSCF particles could be seen distributed on the surface of YSZ scaffold, and even some LSCF particle congeries appeared in some regions (Fig. 5a). The cathode prepared by the LSCF-precursor solution with F127 had relatively few and irregular LSCF particles distributed on the surface of the YSZ scaffold (Fig. 5b). However, the introduction of PVP during the preparation process of cathodes increased the LSCF loading of cathodes. We observed that larger LSCF particles were distributed randomly on the surface of the YSZ scaffold (Fig. 5c), which resulted in cathodes with poor conductivities. The ideal cathode architecture (one with uniform and continuous LSCF particles distributed on the surface of the YSZ scaffold), was obtained after the introduction of DF10 + acetylacetone during preparation (Fig. 5d). This structure had high specific surface area and excellent electrocatalytic activities.

The different effects of surfactants were likely caused by different surface properties. There were many micelles in the LSCF-precursor solutions that contained surfactants, the sizes of these micelles were stable because of the inhibition effects the micelles had on each other. These inhibition effects suppressed the agglomeration of particles that would typically form in solution. DF10 is a fluorocarbon surfactant that can change the wettability of the solid substrate surface. Acetylacetone was used as a solvent to improve the solubility of DF10. Generally, polymer surfactants improve the stability of particles in solutions because the surfactants have long molecular-chain structures. However, long molecular chains can entangle with one another and decrease the

Table 3
Exchange current densities of the LSCF-YSZ composite cathodes with different surfactant at 700 °C and 750 °C in air, each sample had 0.4 mg cm^{-2} of LSCF loading.

Surfactant	Exchange current density i_0 (mA cm^{-2})			
	Low current density		High current density	
	700 °C	750 °C	700 °C	750 °C
DF-10 + acetylacetone	162	258	1107	1223
DF-10	92	132	1076	1191
F127	53	55	1062	1071
No	–	73	1064	1075
PVP	54	194	1065	1183

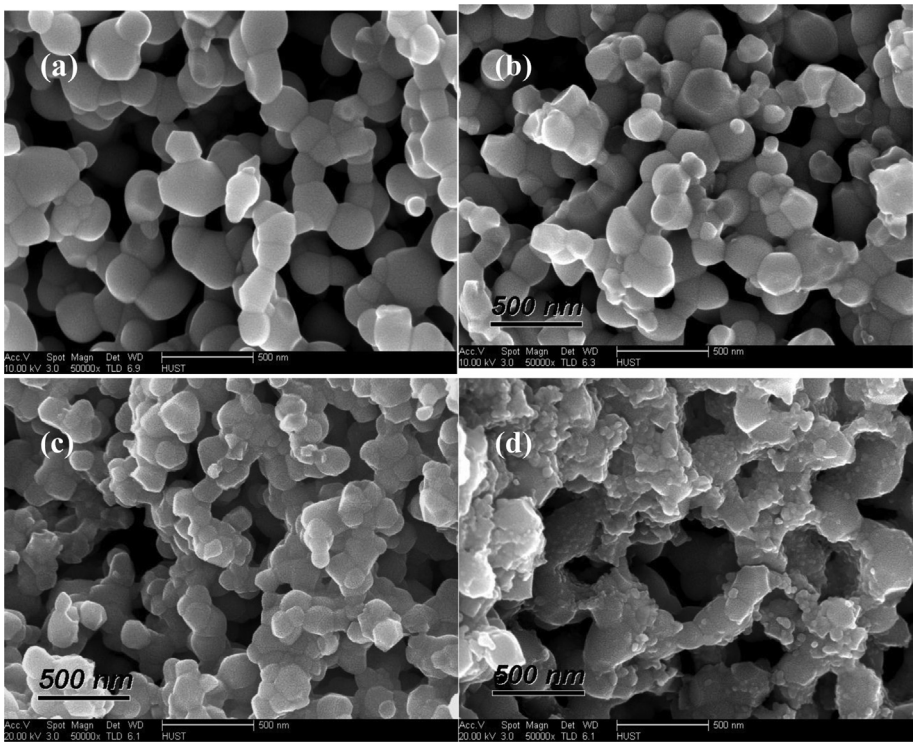

Fig. 5. SEM micrographs of impregnated LSCF-YSZ composite cathodes prepared with different surfactants in LSCF solutions: (a) No; (b) F127; (c) PVP; (d) DF10 + acetylacetone.

dispersion and stability of micelles, causing an increase in the agglomeration of particles. Because of this, the introduction of PVP could have caused the formation of large LSCF particles. Too many LSCF particles can fill the porosity of the cathodes and decrease the activity of oxygen-reduction reactions. For example, when one introduces F127, the ability of LSCF-precursor solutions to access the porous YSZ scaffold during impregnation process becomes difficult. This is because F127 has poor wettability on the surface of the solid YSZ substrate. Even enough LSCF-precursor solutions were dropped onto the surface of the porous YSZ scaffold, few solutions adsorbed the solid YSZ, and few particles were formed after calcination at 800 °C. As a result, fewer LSCF particles in cathodes that were fabricated by LSCF-precursor solutions with F127 led to poor electrochemical activity. The micelles of DF10, as a fluorocarbon surfactant, have strong stability and will block the agglomeration of LSCF particles during the fabrication processes. Therefore, LSCF-precursor solutions in these micelles produce LSCF particles with small uniform sizes, contributing to the result that LSCF-YSZ cathodes fabricated with the introduction of DF10 had excellent electrocatalytic activities.

4. Conclusions

Here, we investigated the effects of LSCF loadings and LSCF particle morphology on the performance of LSCF-YSZ-composite cathodes. We demonstrated that an increase in the LSCF loading initially improved the electrocatalytic activities of LSCF-YSZ cathodes fabricated by impregnation. The exchange current density (i_0) increased with the increase of LSCF loadings showed that the introduction of LSCF phases improved the electrocatalytic activities of LSCF-YSZ cathodes. However, the electrocatalytic activities subsequently decreased after the LSCF loading reached a certain value. The surfactant used in the solution had great effect on the morphology of the LSCF particles. Results of our electrochemical measurements and microstructure analyses showed that the introduction of DF10 + acetylacetone into LSCF-precursor solution during preparation greatly enhance the electrochemical performance of LSCF-YSZ composite cathodes. Our results indicate that the appropriate LSCF loadings and morphology can lead to optimized microstructure with uniform and continuous LSCF particles distributed on the surface of the YSZ scaffold, which gives the LSCF-YSZ composite cathodes an improvement in their electrocatalytic activities.

Acknowledgments

This work was financially supported by the National Natural Science Foundation of China (U1134001), (51102079), China Postdoctoral Science Foundation (2013M540576) and the National “863” Project 2011AA050702. XRD and SEM examinations were assisted by the Analytical and Testing Center of Huazhong University of Science and Technology.

References

[1] L.-W. Tai, M.M. Nasrallah, H.U. Anderson, D.M. Sparlin, S.R. Sehlin, Solid State Ionics 76 (1995) 273–283.
[2] J. Li, S.P. Jiang, in: Solid Oxide Fuel Cells, CRC Press, 2008, pp. 131–177.
[3] S.P. Simner, M.D. Anderson, M.H. Engelhard, J.W. Stevenson, Electrochem. Solid State Lett. 9 (2006) A478–A481.
[4] E.D. Wachsman, K.T. Lee, Science 334 (2011) 935–939.
[5] M.E. Lynch, L. Yang, W.T. Qin, J.J. Choi, M.F. Liu, K. Blinn, M.L. Liu, Energy Environ. Sci. 4 (2011) 2249–2258.
[6] W.G. Wang, M. Mogensen, Solid State Ionics 176 (2005) 457–462.
[7] L.F. Nie, M.F. Liu, Y.J. Zhang, M.L. Liu, J. Power Sources 195 (2010) 4704–4708.
[8] J.M. Vohs, R.J. Gorte, Adv. Mater. 21 (2009) 943–956.
[9] S.P. Jiang, Int. J. Hydrogen Energy 37 (2011) 449–470.
[10] T.Z. Sholklapper, C.P. Jacobson, S.J. Visco, L.C. De Jonghe, Fuel Cells 8 (2008) 303–312.
[11] Z.Y. Jiang, C.R. Xia, F.L. Chen, Electrochim. Acta 55 (2010) 3595–3605.
[12] J. Chen, F.L. Liang, D. Yan, J. Pu, B. Chi, S.P. Jiang, J. Li, J. Power Sources 195 (2010) 5201–5205.
[13] L. Adijanto, R. Kungas, F. Bidrawn, R.J. Gorte, J.M. Vohs, J. Power Sources 196 (2011) 5797–5802.
[14] M. Shah, S.A. Barnett, Solid State Ionics 179 (2008) 2059–2064.

[15] M. Shah, J.D. Nicholas, S.A. Barnett, Electrochem. Commun. 11 (2009) 2–5.
[16] J. Chen, F.L. Liang, B. Chi, J. Pu, S.P. Jiang, J. Li, J. Power Sources 194 (2009) 275–280.
[17] F.L. Liang, J. Chen, S.P. Jiang, B. Chi, J. Pu, J. Li, Electrochem. Solid State Lett. 11 (2008) B213–B216.
[18] S.B. Adler, J. Electrochem. Soc. 149 (2002) E166–E172.
[19] J. Winkler, P.V. Hendriksen, N. Bonanos, M. Mogensen, J. Electrochem. Soc. 145 (1998) 1184–1192.
[20] A. Esquirol, N.P. Brandon, J.A. Kilner, M. Mogensen, J. Electrochem. Soc. 151 (2004) A1847–A1855.
[21] X.J. Chen, S.H. Chan, K.A. Khor, Electrochim. Acta 49 (2004) 1851–1861.
[22] J. Chen, F. Liang, L. Liu, S. Jiang, B. Chi, J. Pu, J. Li, J. Power Sources 183 (2008) 586–589.
[23] S.P. Jiang, Solid State Ionics 146 (2002) 1–22.
[24] J. Fleig, J. Maier, J. Eur. Ceram. Soc. 24 (2004) 1343–1347.
[25] S.B. Adler, Chem. Rev. 104 (2004) 4791–4843.
[26] T.Z. Sholklapper, C. Lu, C.P. Jacobson, S.J. Visco, L.C. De Jonghe, Electrochem. Solid State Lett. 9 (2006) A376–A378.
[27] Z.Y. Jiang, C.R. Xia, F. Zhao, F.L. Chen, Electrochem. Solid State Lett. 12 (2009) B91–B93.
[28] Z.Y. Jiang, Z.W. Lei, B. Ding, C.R. Xia, F. Zhao, F.L. Chen, Int. J. Hydrogen Energy 35 (2010) 8322–8330.
[29] X.Y. Lou, Z. Liu, S.Z. Wang, Y.H. Xiu, C.P. Wong, M.L. Liu, J. Power Sources 195 (2010) 419–424.
[30] B.A. Boukamp, Solid State Ionics 143 (2001) 47–55.
[31] F.L. Liang, J. Chen, J.L. Cheng, S.P. Jiang, T.M. He, J. Pu, J. Li, Electrochem. Commun. 10 (2008) 42–46.